AIMS Materials Science, 3(4): 1623-1631.
DOI: 10.3934/matersci.2016.4.1623
Received: 26 September 2016
Accepted: 08 November 2016
Published: 25 November 2016

http://www.aimspress.com/journal/Materials

Research article

Study on multiple surface crack growth and coalescence behaviors

Masanori Kikuchi *

Department of Mechanical Engineering, Faculty of Science and Technology, Tokyo University of Science, Japan

* **Correspondence:** Email: kik@rs.noda.tus.ac.jp; Tel: +81-4-7124-1501; Fax: +81-4-7123-5782.

Abstract: Interaction of multiple surface cracks is studied by experimental and numerical methods. For experiment, a new method to introduce two surface cracks with different sizes is developed. Using this technique, four point bending fatigue tests including coalescence process of two surface cracks are conducted by changing crack sizes of two cracks. Crack growing process is studied by introducing beach marks. Change of crack shapes and coalescence behaviors are observed clearly. Locations of crack coalescence change due to the change of crack sizes. Same problem is simulated by using S-FEM. Two models are simulated. One is Crack coalescence model, and another is Virtual single rack model. Virtual single crack model is based on the proximity rule of JSME maintenance code. Results of both models are compared with those of experiment. Results show the availability of numerical methods to predict coalescence process of two surface cracked specimens. It is also shown that JSME code is useful to simulate coalescence problem.

Keywords: multiple surface crack; coalescence; S-FEM

1. Introduction

Ensuring the integrity of mechanical components is one of the most important problems in the industrial manufacturing process. Every mechanical component suffers damage over long-term use, and the accumulation of damage ultimately results in fatigue fracture. To prevent final fracture, fatigue cracks should be detected, and appropriate maintenance should be performed. For this purpose, technology that can predict fatigue crack growth is important. The finite element method (FEM) is the most powerful tool for such predictions. However, a re-meshing process is required to model of growing fatigue crack, and it is very difficult and time-consuming, especially for three-dimensional (3D) crack models. Researchers have recently developed many numerical techniques,

including the extended FEM (X-FEM) [1], the dual boundary element method (BEM) [2], the element-free Galerkin method [3], and the free mesh method [4]. Authors employed S-FEM, proposed by Fish et al. [5], and developed a fully automatic system for crack growth simulation. Several types of complicated crack growth problems have been simulated, and the applicability of the S-FEM has been verified [6–9].

It is important to validate the numerical results of such simulations. For this purpose, comparison of the numerical results with those of experiment is necessary. In this paper, interaction behaviors of multiple surface cracks are studied by experiment and numerical simulations. Test specimen with two surface cracks of different sizes are used for fatigue test, and crack growth and coalescence processes are observed experimentally. These processes are re-produced by numerical method, by S-FEM, and proximity rule by JSME maintenance code [10] is discussed.

2. Fatigue Test of Two Surface Cracked Specimen

2.1. Test Specimen

Test material is Aluminum alloy A7075-T6. Young's modulus of this material is 71.7 GPa, and Poisson's ration is 0.3. Two surface cracks are introduced into a plate and four points bending fatigue tests are conducted.

Figure 1(a) shows size and shape of test specimen. Two protuberances are made on one side of the plate, and initial notches are introduced by EDM (Electric Discharged Machining) here. Sizes of initial notch are shown in Figure 1(b). Initial cross section of this specimen is shown in Figure 1(c). Four points bending cyclic load is subjected to this specimen. The maximum load is 25 kN, stress ratio is 0.1 and cyclic frequency is 20 Hz. By these conditions, two surface cracks are generated from initial notches and grow in the specimen, as shown in Figure 2. Finally, by cutting off these protuberances, plate specimen with different sized two surface cracks is obtained. By changing X_1 and X_2 values, width of protuberance, and S value, distance between two protuberances, as shown in Figure 1(c), it is possible to control final surface crack sizes and distance between two cracks. In this study, 4 specimens are prepared. Table 1 shows X_1, S and X_2 values for these specimens. X_1 and S values are kept constant, and only X_2 is changed in four cases. They are called Case1 to Case 4 in the following. In Case 1, sizes of two surface cracks are same, and right side surface crack size increases gradually from Case 2 to Case 4.

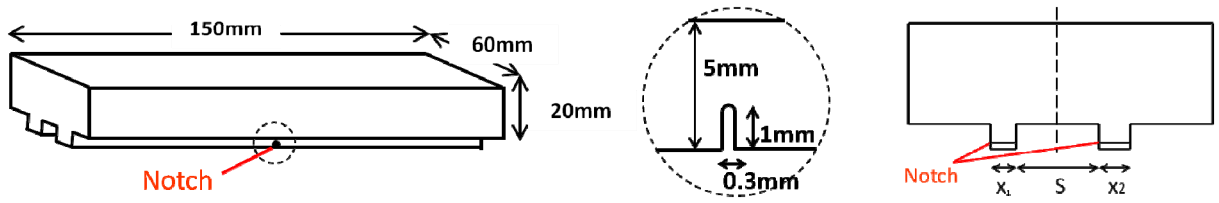

(a) Front view (b) Notch (c) Side view

Figure 1. Introduction of initial notches to a plate with two protuberance.

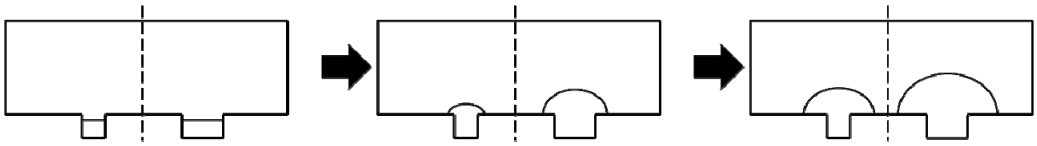

Figure 2. Growing process of two surface cracks.

Table 1. Protuberance size [mm].

	X_1	S	X_2
Case1	3	7	3
Case2	3	7	5.5
Case3	3	7	8
Case4	3	7	13

Four points fatigue tests are conducted using these specimens. Figure 3 shows loading positions of fatigue tests. Maximum load is 25 kN, and stress ratio, R, is 0.1. Beach marks are introduced during fatigue test by changing R value as 0.8. For each Case, 5 specimens are tested. In the following, test results of one specimen in five tests are shown for each Case. Coordinate system, x-y-z, is set as shown in this figure, which is used in the following explanation of test results.

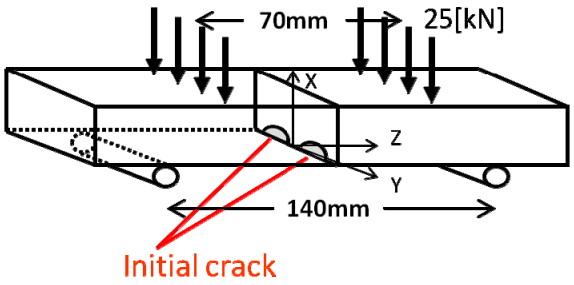

Figure 3. Four points bending test.

2.2. Test results

Figure 4 shows test results. Beach marks in each specimen are shown by dark lines. Red lines indicate first beach marks from initial notch, and they are used as the initial crack in the following numerical simulations. Number of cycles for each beach mark is measured and they are compared with numerical simulations.

In Case 1 specimen, initial two cracks are nearly same size, and crack growths occur symmetrically, and coalescence occurs at the center of the specimen. Just after the coalescence, single crack has saddle point at the coalesced location. But crack growth occurs rapidly at this location, and crack shape becomes single large semi-elliptical surface crack. After then, beach marks show that crack growth rate at surface is larger than that at the bottom of the crack.

In Case 2 specimen, right side surface crack is larger than left side one. Then, coalescence

occurs near to left side crack. This is clear in Cases 3 and 4 specimens, where right side crack is much larger than left side one. Location of coalescence and growth is observed in these specimens as a curved line. In Case 4, crack growth occur mainly in right side crack, and crack growth amount of left side one is very small before coalescence. Finally, every cracks become large semi-elliptical surface cracks.

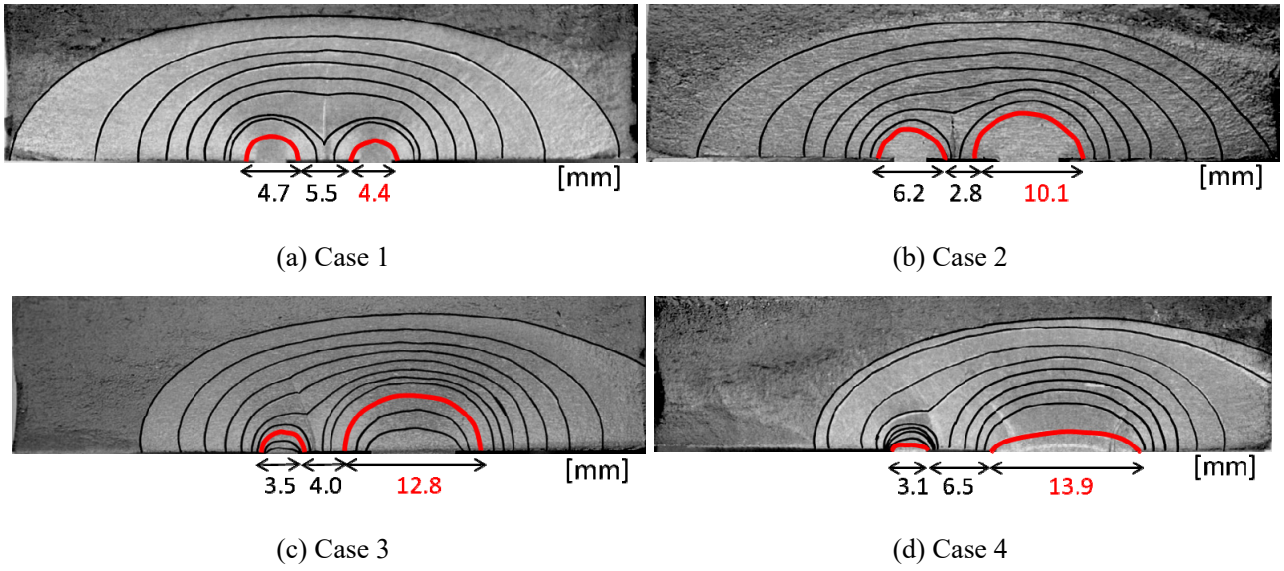

(a) Case 1 (b) Case 2

(c) Case 3 (d) Case 4

Figure 4. Fracture surface.

3. Crack Growth and Coalescence Simulation Using S-FEM

3.1. Brief Introduction of S-FEM

S-FEM is originally proposed by J. Fish [5]. As shown in Figure 5, a structure with a crack is modeled by global mesh and local mesh. Global area, Ω_G, does not include a crack, and course mesh is used for the modeling of global area. A crack is modeled in local area, Ω_L, using fine mesh around crack tip. Local area is superimposed on global area and full model is made. In each area, displacement function is defined independently. In overlapped area, displacement is expressed by the summation of displacement of each area. To keep the continuity at the boundary between global and local area, Γ^{GL}, displacement of local area is assumed to be zero as shown in the following equation.

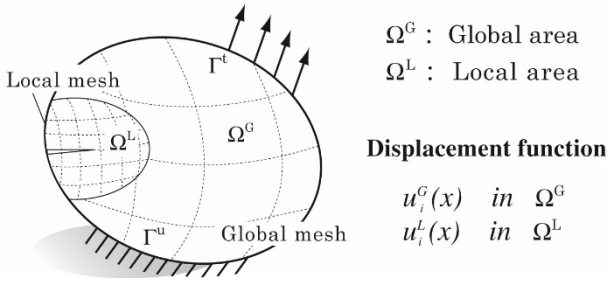

Figure 5. Concept of S-FEM.

$$u_i = \begin{cases} u_i^G & i \in \Omega_G - \Omega_L \\ u_i^G + u_i^L & i \in \Omega_L \\ u_i^L = 0 & i \in \Gamma^{GL} \end{cases} \tag{1}$$

The derivatives of displacements can be written in the same way. These displacement functions are applied to virtual work principle, as shown in Eq. (2), and the final matrix form of S-FEM is obtained as shown in Eq. (3)

$$\begin{aligned} &\int_{\Omega^G} \delta u_{i,j}^G D_{ijkl} u_{k,l}^G d\Omega + \int_{\Omega^L} \delta u_{i,j}^G D_{ijkl} u_{k,l}^L d\Omega \\ &+ \int_{\Omega^L} \delta u_{i,j}^L D_{ijkl} u_{k,l}^G d\Omega + \int_{\Omega^L} \delta u_{i,j}^L D_{ijkl} u_{k,l}^L d\Omega = \int_{\Gamma^t} \delta u_i^G t_i d\Gamma^{tG} \end{aligned} \tag{2}$$

$$\begin{bmatrix} [K^{GG}] & [K^{GL}] \\ [K^{LG}] & [K^{LL}] \end{bmatrix} \begin{Bmatrix} u^G \\ u^L \end{Bmatrix} = \begin{Bmatrix} t^G \\ 0 \end{Bmatrix} \tag{3}$$

In Eq. (3), $[K^{LG}]^T = [K^{GL}]$, and the stiffness matrix is symmetric. $[K^{GL}]$ expresses the relationship between local and global areas. By calculating this term with high accuracy, accurate FEM results are obtained. By solving Eq. (3), both displacement fields of local and global areas are obtained simultaneously. The detail of the theory was presented in the literature of one of the authors [6].

For fatigue crack growth simulation, re-meshing process is needed for growing crack configuration. In S-FEM, local area including crack is modeled as local mesh, and easy to re-mesh this area due to crack growth. This method models one crack by one local mesh, and is easy to simulate multiple crack problems, because multiple local meshes are made independently to each other. As a result, if multiple crack tips become very near to each other, there is no difficulties for re-meshing process, and interaction effect of multiple cracks problem is simulated easily and with high accuracy. Figure 6(a) shows whole mesh including global mesh and local mesh, and local mesh is shown in Figure 6(b). This is just after coalescence of Case 3 specimen. In S-FEM, re-meshing process is needed only for local mesh, which is a small part of whole structure. Then it becomes very easy to follow growing crack shape by fatigue loading. For re-meshing, auto-meshing technique is used.

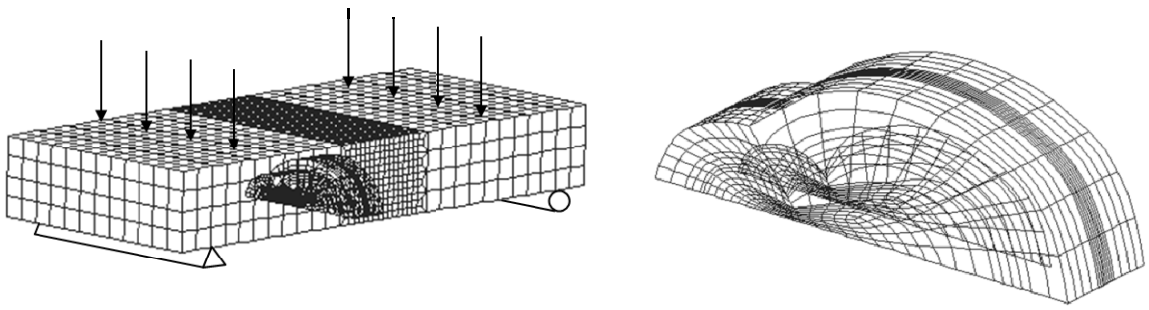

(a) Mesh model (b) Crack model

Figure 6. Global and local meshes.

3.2. Crack Growth and Coalescence Simulation

For fatigue crack growth simulation, Paris' law [11], shown in Eq. (4), is used where C and n are material constants. For A7075-T6, $C = 2.29 \times 10^{-4}$ and $n = 2.88$ are used. Stress intensity factor is evaluated by VCCM [12], and stress intensity factor, ΔK_I, is obtained.

$$\frac{da}{dN} = C(\Delta K_I)^n \tag{4}$$

Two kinds of crack growth and coalescence analyses are conducted. One is shown in Figure 7(a), from (i) to (vii). At first, (i) two surface cracks are assumed, and (ii) crack growth analyses are conducted for these cracks. When two cracks become very near to each other, (iii) coalescence of both cracks is assumed, and single crack model is made as local mesh. This coalescence process is shown in Figure 8(a). By assuming a very little crack growth to overlapping direction, a new crack front is made by the enveloping line, as shown by red line in Figure 8(a). After then, from (iv) to (vii), crack growth simulation of this single surface crack is conducted, and finally, large semi-elliptical surface crack is generated. This process is called "Coalesced crack model". The second simulation process is shown in Figure 7(b) from (i) to (vii). Processes (i) and (ii) are same as first case. In this case, coalescence model is made based on proximity rule of JSME. JSME rule defines a virtual single semi-elliptical crack as a coalesced crack, as shown in Figure 8(b), where depth of this crack is same as deeper single crack before coalescence, and width of it is the summation of two surface cracks. Local model of this new single crack is shown in (iii) of Figure 7(b). Then crack growth simulation is conducted from (iv) to (vii). This is called "Virtual single crack model".

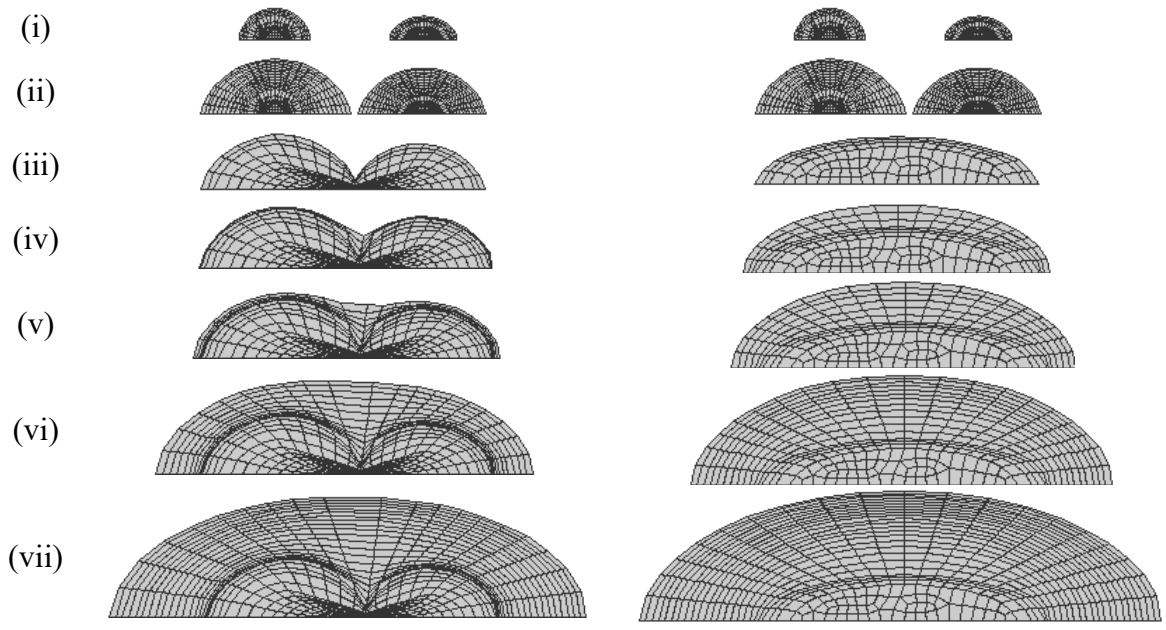

(a) Coalesced crack model (b) Virtual single crack model

Figure 7. Crack model.

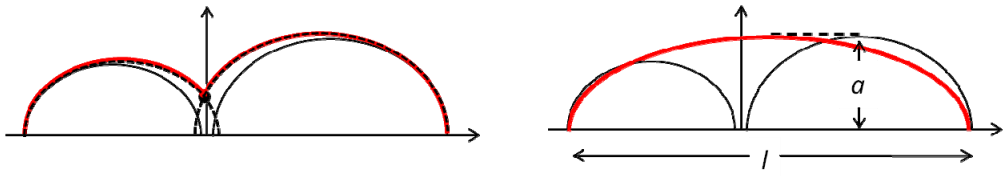

(a) Coalesced crack model (b) Virtual single crack model

Figure 8. Method of just after coalescence.

4. Comparison on Numerical Results with Experimental Ones

Figure 9(a) shows comparison of crack front configurations by experiment and Coalesced crack model for Case 1. Five specimens are tested in fatigue tests for each Case, but results shown in these figures are plotted using data from one of them. Both results show similar ones at coalesced location of two cracks. Just after coalescence, sharp V-shape is made, but crack growth at this location occurs very rapidly, and becomes one single semi-elliptical surface crack. Figure 9(b) shows comparison results by Virtual single crack model and experiment. By this model, crack growing process is well simulated. The difference from Figure 9(a) is there is no sharp V-notch shape after coalescence. As Case 1 is symmetrical case, crack growth also occurs symmetrically in both results. It is also shown that crack lengths at surface by numerical simulations are larger than that by experiment when crack depths of both results are similar to each other. This is due to crack closure effect, which is discussed in authors' previous paper [13].

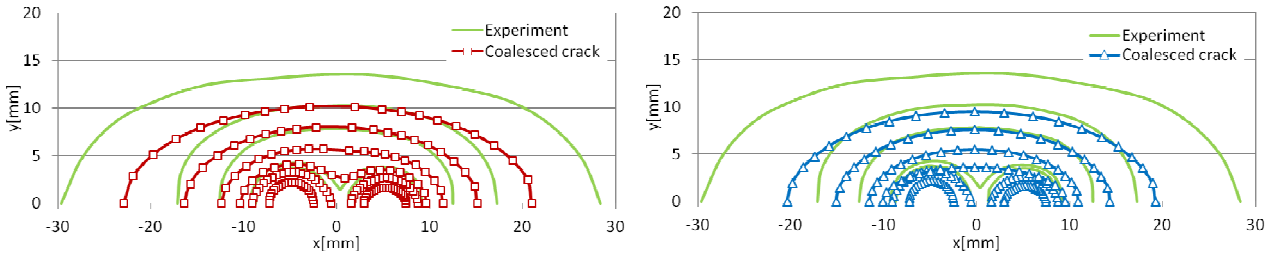

(a) Coalesced crack model (b) Virtual single crack model.

Figure 9. Comparison of crack shapes of numerical results with experimental ones for Case 1.

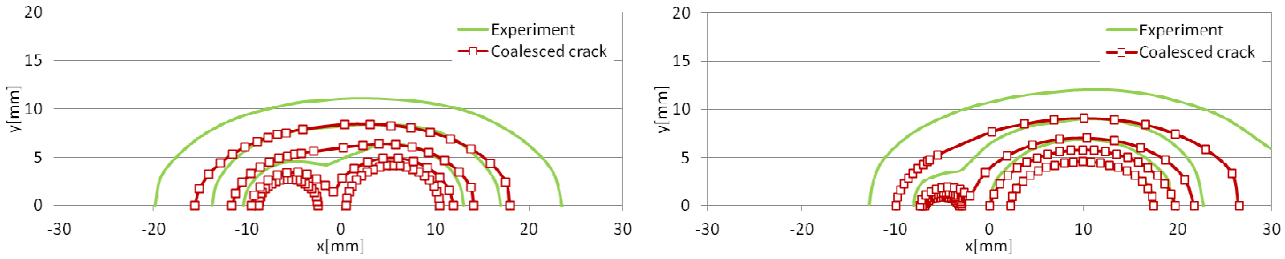

(a) Case 2 (b) Case 4

Figure 10. Comparison of crack shapes of Coalesced crack model with experimental ones.

Figure 10(a) shows comparison of results by Coalesced crack model and experiment for Case 2, and Figure 10(b) shows those for Case 4. In all results, coalescence processes are well re-produced by Coalesced crack model. In Case 4, crack growth of left side crack is very small comparing with right side crack, which agrees with experimental result shown in Figure 4(d). As the difference of two crack sizes increase, the coalescence location moves to smaller crack side, and main crack growth process is by larger crack.

Figure 11(a)–(d) show comparison of crack growth rate by numerical simulation and experiment. In these figures, the ordinate is *dc/dN*, which means crack growth rate along specimen surface. In these figures, experimental data are average of five test specimens. Both numerical results, by Coalesced crack model and Virtual single crack model, show similar results. It means that the crack coalescence prediction is well conducted using proximity rule of JSME, which shows availability of JSME code for multiple surface crack problems. By comparing with experimental results, it is noticed that in Case 1, numerical results estimate crack growth rate slightly non-conservatively, but difference between numerical simulation and experiment is small. By considering the data scatter in fatigue tests, it can be concluded that crack growth rate including coalescence process is well estimated by numerical methods.

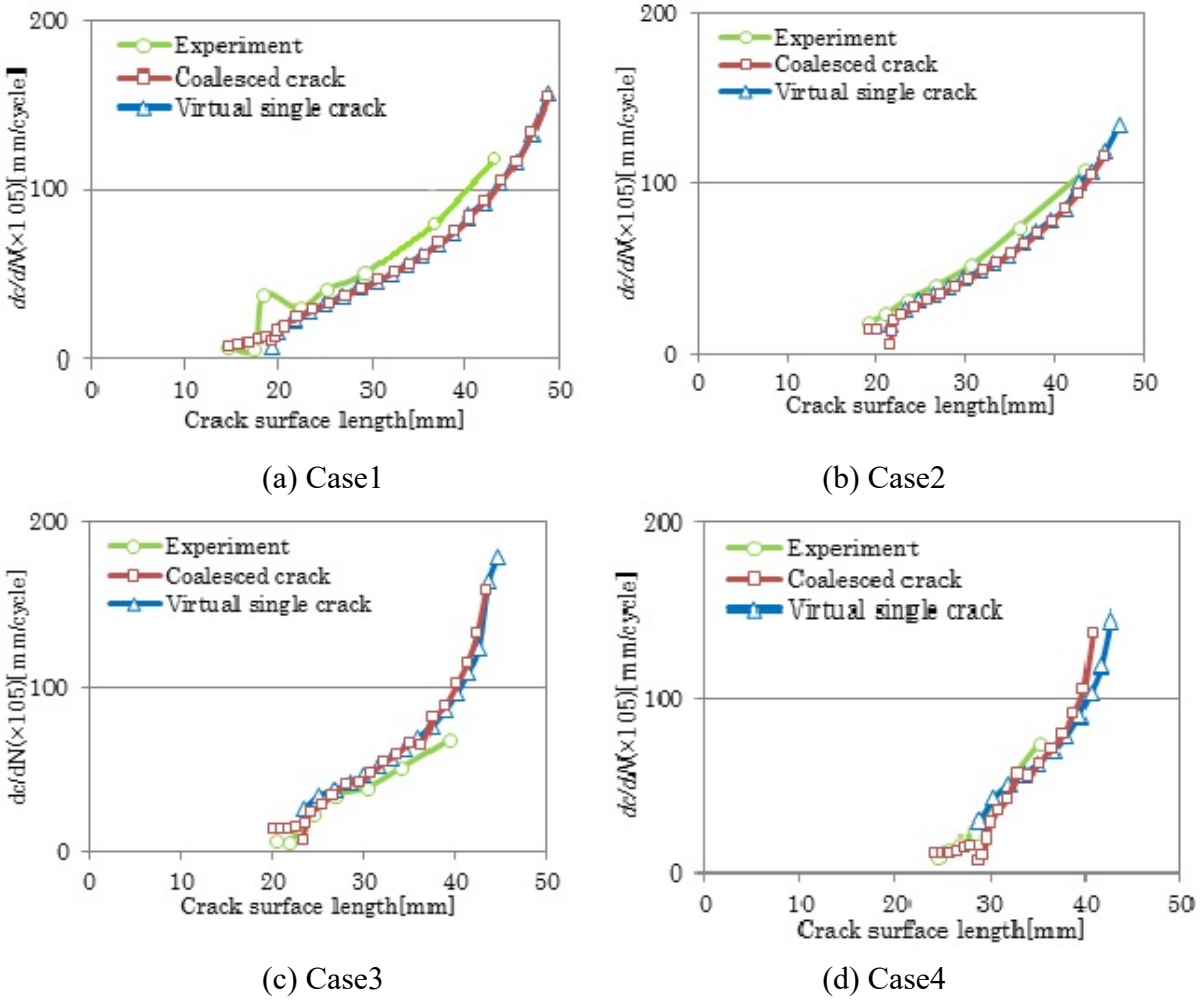

(a) Case1 (b) Case2

(c) Case3 (d) Case4

Figure 11. Crack growth rate.

5. Conclusion

Crack coalescence process of two surface cracks is studied by experiment and numerical simulation. In experiments, a new technique to obtain two surface cracked specimen with different crack sizes is developed, and its' usefulness is shown. This technique can be applied for more than 3 surface cracks problem. By numerical simulations, it is concluded that both models, Coalesced crack model and Virtual single crack model, well predict crack coalescence process. It is important to know that the proximity rule of JSME gives good estimation of crack coalescence process.

Conflict of Interest

The author declares no conflicts of interest regarding this paper.

References

1. Belytschko T, Black T (1999) Elastic crack growth in finite elements with minimal remeshing. *Int J Numer Meth Eng* 45: 601–620.
2. Mi Y, Aliabadi MH (1992) Dual boundary element method for three-dimensional fracture mechanics analysis. *Eng Anal Bound Elem* 10: 161–171.
3. Belytschko T, Lu YY (1994) Element-free Galerkin methods. *Int J Numer Meth Eng* 37: 229–256.
4. Yagawa G, Yamada T (1996) Free mesh method: A new meshless finite element method. *Comput Mech* 18: 383–386.
5. Fish J, Markolefas S (1993) Adaptive s-method for linear elastostatics. *Appl Numer Math* 14: 135–164.
6. Okada H, Endoh S, Kikuchi M (2005) On fracture analysis using an element overlay technique. *Eng Fract Mech* 72: 773–789.
7. Kikuchi M, Wada Y, Takahashi M, et al. (2008) Fatigue Crack Growth Simulation using S-Version FEM. ASME 2008 Pressure Vessels and Piping Conference, Chicago, Illinois, USA.
8. Maitireyimu M, Kikuchi M, Geni M (2009) Comparison of Experimental and Numerically Simulated Fatigue Crack Propagation. *J Solid Mech Mater Eng* 3: 952–967.
9. Shintaku Y, Iwamatsu F, Suga K, et al. (2015) Simulation of Stress Corrosion Cracking in In-Core Monitor Housing of Nuclear Power Plant. *J Press Vess Tech* 137: 041401–041401-13.
10. JSME S Nal-2004 (2004) Codes for Nuclear Power Generation Facilities: Rule of Fitness-for-Service for Nuclear Power Plants, Tokyo, Japan.
11. Paris P, Erdogan F (1963) A critical analysis of crack propagation laws. *J Basic Eng* 85: 528–533.
12. Rybicki KF, Kanninen MF (1997) A finite element calculation of stress intensity factors by a modified crack closure integral. *Eng Fract Mech* 9: 931–938.
13. Kikuchi M, Maigefeireti M, Sano H (2010) Closure Effect of Interaction of Two Surface Cracks under Cyclic Bending. ASME 2010 Pressure Vessels and Piping Division/K-PVP Conference, Bellevue, Washington, USA.

AIMS Press